JMEPEG (1994) 3:490-495

Intelligent Recognition of Drill Wear States

T.I. Liu, W.Y. Chen, and E.J. Ko

Both thrust force and vertical acceleration in the drilling process can be used as indirect indices to classify the drill wear conditions. In this work, these two indices are used as the input vector of the neural networks; the neural network outputs are the wear states.

Neural networks simulate the human brain and can learn from experience. They are adaptive and intelligent. The learning process of the neural networks used in this work was conducted using the back propagation technique.

Different architectures of neural networks have been employed and compared. The results of using one kind of sensor and the results based on sensor fusion and neural networks are discussed and compared. The neural networks have very impressive performance and can achieve a success rate of 90% for on-line recognition of drill wear states.

Keywords

drill wear, neural networks, sensor fusion, thrust force, vertical acceleration

1. Introduction

ON-LINE recognition of tool wear is essential for the factory of the future (Ref 1, 2, 3). Researchers have developed on-line classification systems for drill wear to facilitate factory automation, yet intelligence should be integrated into the current systems to further improve their performance.

Researchers pointed out that the drill condition can be detected indirectly by measuring the thrust force (Ref 4, 5, 6). In addition, the drill wear can be sensed indirectly by measuring the acceleration (Ref 5, 7, 8). Sensor fusion was used to integrate both thrust and accelerations so that two kinds of signals could be used simultaneously to indicate the drill wear conditions (Ref 5). This system provides more information about drill wear conditions and is more reliable.

Artificial neural networks were used to effectively process the information contained in the multiple sensory signals. Drill wear conditions were classified into different wear categories:

I. Initial wear
II. Slight wear
III. Moderate wear
IV. Severe wear
V. Worn-out

In section 2, artificial neural networks are briefly described. In section 3, experimentation is illustrated in detail. The learning process and on-line recognition of drill wear conditions is discussed in section 4. The on-line recognition scheme based on only one type of sensor and the on-line system using sensor fusion as well as artificial neural networks are also discussed and compared in section 4.

T.I. Liu, W.Y. Chen, and **E.J. Ko,** Department of Mechanical Engineering, California State University-Sacramento, Sacramento, CA 95819-6031, USA

2. Artificial Neural Networks

Artificial neural networks simulate biological nervous systems and are referred to as parallel distributed processing. Artificial neural networks consist of a number of computational units known as neurons connected with a larger number of communicational links. These neurons have a pattern of connectivity among them, the knowledge of which can be represented by the strength of the connections. The pattern of interconnections known as weights is not fixed. Instead, the weights can be modified based on the experience. Hence the system can learn from this experience and is intelligent (Ref 9, 10, 11).

Artificial neural networks can make decisions based on incomplete and noisy information. This system also can calculate its outputs very quickly. These features enable this technique to be used successfully in computer vision and process modeling (Ref 12, 13, 14). This technique is also a candidate for the recognition of tool wear states. In recent years, artificial neural networks were applied to detect the tool wear in machining operations; the results are very encouraging (Ref 2, 15). In this paper, feedforward neural networks were used for on-line drill wear recognition.

2.1 *Feedforward Neural Networks*

Feedforward neural networks consist of the input layer, the output layer, and the hidden layers between them. The information contained in the input is recoded into an internal representation by the hidden units that perform the mapping from input to output. Each unit in this architecture can send its output to the units on the higher layer only and receive its input from the lower layer. Figure 1 shows a typical feedforward neural network that consists of three layers. Each node represents a nonlinear sigmoid function in the form of

$$O_j = \frac{1}{\{\,1 + \exp[-(I_j + \theta_j)]\,\}} \quad \text{(Eq 1)}$$

where $I_j = \Sigma\, W_{ji}\, O_i$

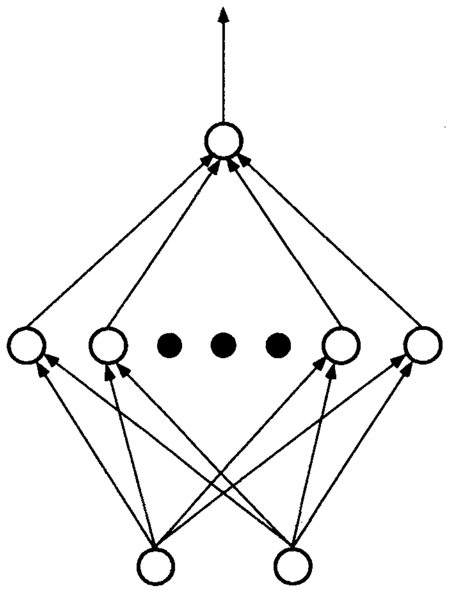

Fig. 1 Neural network structure

In the above equations, I_j is the input of the current node, O_j is the output of the current node, O_i is the output of the node on the preceding layer, and θ_j is the threshold of the current node. Obviously, all the node outputs range between 0 and 1 as indicated in Eq 1. Hence all the data should be normalized before being applied to the neural networks so that they are confined between 0.1 and 0.9. All the data, d, are normalized as d_n according to:

$$d_n = [\ (0.9 - 0.1)/(d_{\max} - d_{\min})\ ]\ (d - d_{\min}) + 0.1 \qquad \text{(Eq 2)}$$

In Eq 2, $d_{\max}$ and $d_{\min}$ are the maximum and minimum values of the data, d, respectively.

2.2 *Learning Process*

The neural networks need to be trained in a learning process before they are applied for on-line classification of drill wear. The learning process starts by assigning random values to the weights, W_{ji}, and thresholds, θ_j. The output is obtained by a forward pass starting from the input vector. Each node calculates its output by summing its weighted inputs and using the summation as the argument for a nonlinear function shown in Eq 1. The estimated output at the output layer is quite different from the desired output because the values of the weights and the thresholds are randomly assigned. In order to minimize the estimation error, the back propagation technique is employed to adjust all the weights and thresholds.

The back propagation technique uses the difference between the desired output and the estimated value to adjust the weights and thresholds. The error ε is propagated backwards using the generalized delta rule:

$$\delta_O = \varepsilon O_O\,(1 - O_O) \qquad \text{(Eq 3)}$$

for nodes of the output layer, and

$$\delta_j = O_j\,(1 - O_j)\ \Sigma \delta_k W_{kj} \qquad \text{(Eq 4)}$$

for all other nodes.

In the above equations, the indexes i, j, and k stand for the preceding, the current, and the next layers. The weights, W_{ji}, and the thresholds, θ_j, can be modified as:

$$W_{ji}\,(n+1) = W_{ji}(n) + \eta\ \delta_j\, O_i \qquad \text{(Eq 5)}$$

$$\theta_j\,(n+1) = \theta_j\,(n) + \eta\ \delta_j \qquad \text{(Eq 6)}$$

where η is the learning rate and n is the current number of iterations. Obviously the weight and the threshold will be increased if the estimated value from the node is smaller than the desired output, and vice versa.

The above procedure can be used to determine the error and then to adjust the weights and thresholds. This learning process can be carried out until the estimated output is sufficiently close to the desired output. After the weights and thresholds have been adjusted for one set of training data, additional training sets can be used to further adjust all the weights and thresholds of the neural network. This learning process is finally terminated when the error becomes smaller than a predetermined error limit.

After the feedforward neural networks have been trained in the learning process, they can be used for other sets of operating data. When new inputs are presented to the neural networks, the output will be predictable. If the operating conditions are governed by the same underlying mechanism, the performance of the neural networks should be satisfactory.

3. Experimentation

The observations in Table 1 were made during drilling 107.7-mm × 6.35-mm oil holes into nodular cast-iron crankshafts using an optimum multifacet drill (MFD) as shown in the Appendix 1 (Ref 16). The spindle speed was 2100 rpm, and the feedrate was 0.178 mm/rev.

The vertical acceleration during drilling was measured by a quartz accelerometer. The signals were amplified by a dual mode amplifier. The drilling thrust was measured by a strain gage dynamometer. The signals were amplified by a strain gage amplifier. Both signals were measured when the drilling depth reached 12.7 mm (0.5 in.). The signals were filtered by low pass filters with a cutoff frequency of 100 Hz. The signals were recorded by a cassette data recorder and monitored by the oscilloscope. The experimental setup is shown in Fig. 2, and the data for the training purpose are shown in Table 1.

Table 1 Percent increases of the vertical acceleration and the thrust of the training vectors
Spindle speed: 2100 rpm. Feedrate: 0.178 mm/rev.

	Test No.	Category I measured (mv)	%	Category II measured (mv)	%	Category III measured (mv)	%	Category IV measured (mv)	%	Category V measured (mv)	%
Vertical acceleration	1	142	100	180	127	185	130	210	148	226	159
	2	145	100	190	131	193	133	219	151	236	163
	3	133	100	157	118	161	121	180	135	197	148
	4	138	100	175	127	177	128	196	142	201	146
Thrust	1	265	100	281	106	286	108	313	118	363	137
	2	268	100	276	103	281	105	308	115	340	127
	3	251	100	291	116	299	119	344	137	374	149
	4	265	100	281	106	315	119	345	130	371	140

Table 2 Percent increases of the vertical acceleration and the thrust for on-line tests
Spindle speed: 2100 rpm. Feedrate: 0.178 mm/rev.

	Test No.	Category I measured (mv)	%	Category II measured (mv)	%	Category III measured (mv)	%	Category IV measured (mv)	%	Category V measured (mv)	%
Vertical acceleration	1	143	100	160	112	167	117	199	139	203	142
	2	138	100	170	123	171	124	201	146	207	150
	3	134	100	154	115	158	118	184	137	204	152
	4	128	100	170	133	175	137	186	145	191	149
	5	130	100	169	130	170	131	181	139	200	154
	6	132	100	164	124	168	127	191	145	205	155
Thrust	1	252	100	262	104	280	111	333	132	363	144
	2	257	100	278	108	393	114	324	126	347	135
	3	255	100	296	116	301	118	334	131	360	141
	4	249	100	266	107	291	117	299	120	356	143
	5	266	100	279	105	285	107	303	114	346	130
	6	263	100	289	110	292	111	345	131	352	134

Additional data listed in Table 2 were taken under the same operating conditions. These data were used for on-line tests for recognition of drill wear states.

The flank wear area shown in Tables 3 and 4 is an index of the drill wear. A vision system was used to measure the flank wear (Ref 5).

4. On-Line Classification of Drill Wear Based on Artificial Neural Networks

4.1 *On-Line Recognition using Sensor Fusion and Artificial Neural Networks*

In order to observe the drill wear conditions more effectively, two kinds of signals were used: the vertical acceleration and the drilling thrust. To process these data so that they are dimensionless, the percent increases of the peak-to-peak amplitude of vertical acceleration and the drilling thrust were used, as shown in Tables 1 and 2 and Fig. 3 and 4. These increases were normalized according to Eq 2 and then used as two inputs on the input layer of the neural networks.

On the output layer were the drill wear conditions, which were classified, based on drill wear area measurements, into five categories. Category I, initial wear, means the worn area is under 270 nm^2. Category II, slight wear, means the worn area is between 270 nm^2 and 333 nm^2. Category III, moderate wear, means the worn area is between 333 nm^2 and 474 nm^2. Category IV, severe wear, means the worn area is between 474 nm^2 and 658 nm^2. Category V, worn-out condition, means the worn area is larger than 658 nm^2. Again, the drill wear conditions were normalized so that they can be presented to the output layer of the neural networks.

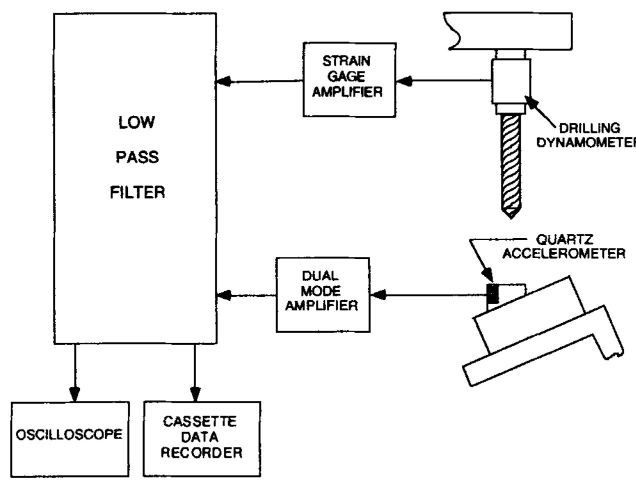

Fig. 2 Experimental setup

A total of 20 training sets were used in the learning process. The learning rate used is 0.1, and the error limit used to stop the iterations in back propagation is under 0.01. Fifteen different

Table 3 Progression of the flank wear area of the optimum crankshaft MFD measured by the new vision system in the learning process

Spindle speed: 2100 rpm. Feedrate: 0.178 mm/rev

Test No.	Category I, nm^2	Category II, nm^2	Category III, nm^2	Category IV, nm^2	Category V, nm^2
1	212.90	296.07	361.29	529.03	722.58
2	251.61	303.45	419.35	600.00	819.35
3	225.37	293.64	379.51	558.76	763.92
4	210.45	288.17	362.49	528.33	714.21

Table 4 Progression of the flank wear area of the optimum crankshaft MFD measured by the new vision system for on-line tests

Spindle speed: 2100 rpm. Feedrate: 0.178 mm/rev

Test No.	Category I, nm^2	Category II, nm^2	Category III, nm^2	Category IV, nm^2	Category V, nm^2
1	238.61	301.28	404.23	584.51	800.00
2	140.82	271.92	318.94	494.54	664.51
3	229.96	290.54	386.76	565.31	774.19
4	218.14	286.24	370.87	544.62	748.39
5	168.81	284.93	347.69	526.12	696.77
6	262.53	309.11	428.17	612.90	828.66

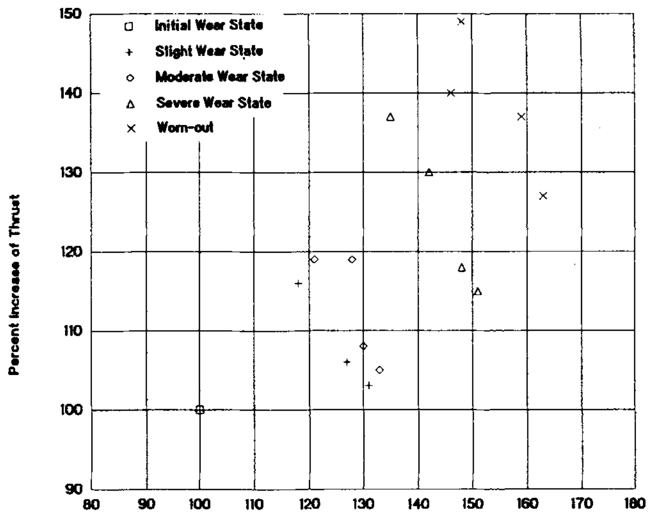

Fig. 3 Training sets in the learning process

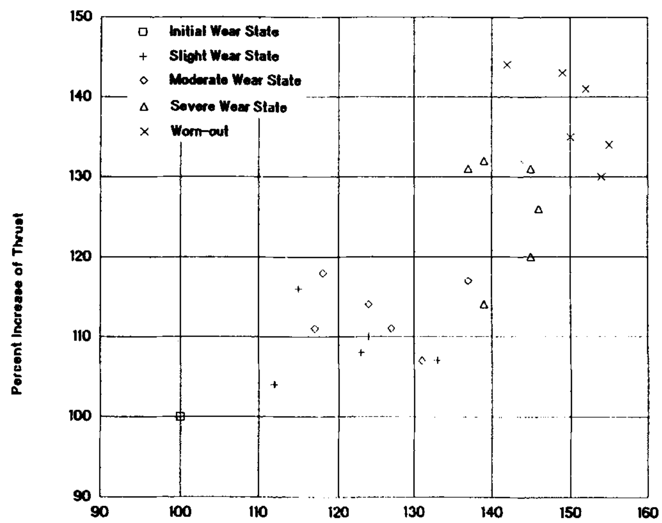

Fig. 4 Data sets for on-line tests

feedforward neural networks were trained in the learning process using the data shown in Tables 1 and 3 as input and output, respectively.

After the learning process, the neural networks were used for on-line recognition of the drill wear. The data shown in Tables 2 and 4 were used for on-line tests; results are in Fig. 5 and Table 5. The rate of success for on-line drill wear recognition ranges from 80.3% to 90%. Nine out of fifteen different neural network structures achieve a success rate of 90%.

4.2 *Justification of Sensor Fusion*

As shown in Fig. 3, the projections of the data on both the horizontal and the vertical axis overlap. It is quite difficult to distinguish the wear states in the overlapping ranges if only a single type of sensor is used. Sensor fusion was used in this work because it can observe the drill conditions from different viewpoints and offer more information about the drill wear.

Suppose only a single type of sensor is employed, and the average values of the maximum and the minimum of two adjacent categories shown in Table 1 are used as boundaries. For example, if only percent increase in drilling thrust is used as a wear index, the maximum value in category III is 119% while the minimum value in category IV is 115%. The average of these two values, 117%, is used to be the boundary between these two categories.

Using the above criteria for on-line classification, there are seven misclassifications out of thirty wear states if only percent increase of peak-to-peak amplitude of vertical acceleration is used, a 76.7% rate of success. There are also seven misclassifi-

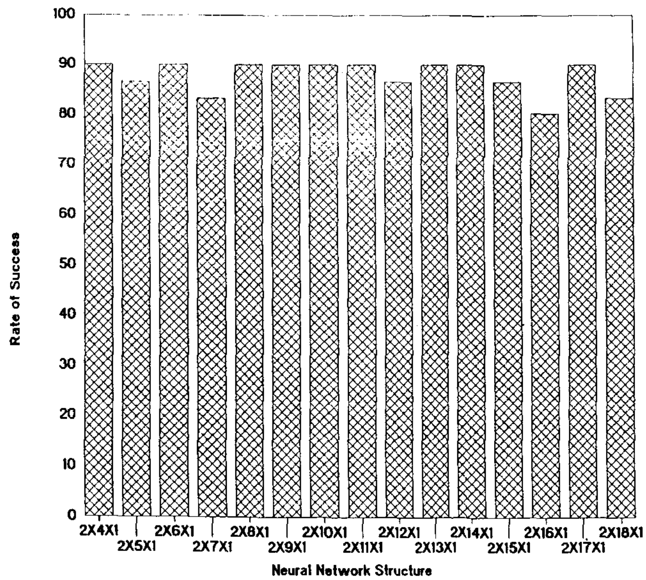

Fig. 5 Effects of neural network structure to the performance

Table 5 Effects of neural network structure

Neural network structure	Rate of success, %
2×4×1	90.0
2×5×1	86.6
2×6×1	90.0
2×7×1	83.3
2×8×1	90.0
2×9×1	90.0
2×10×1	90.0
2×11×1	90.0
2×12×1	86.6
2×13×1	90.0
2×14×1	90.0
2×15×1	86.6
2×16×1	80.3
2×17×1	90.0
2×18×1	83.3

cations if only thrust is used, a 76.7% rate of success. Obviously, sensor fusion and neural networks can greatly enhance the reliability of the on-line drill monitoring system.

5. Conclusions

Based on the work presented in this paper, the reliability of an on-line drill wear recognition system can be greatly improved by using sensor fusion and artificial neural networks. The rate of success for on-line drill wear recognition is only 76.7% by using either only force sensor or only acceleration sensor. However, the performance of the intelligent drill wear recognition system using sensor fusion and neural networks is very impressive with a rate of success of up to 90%.

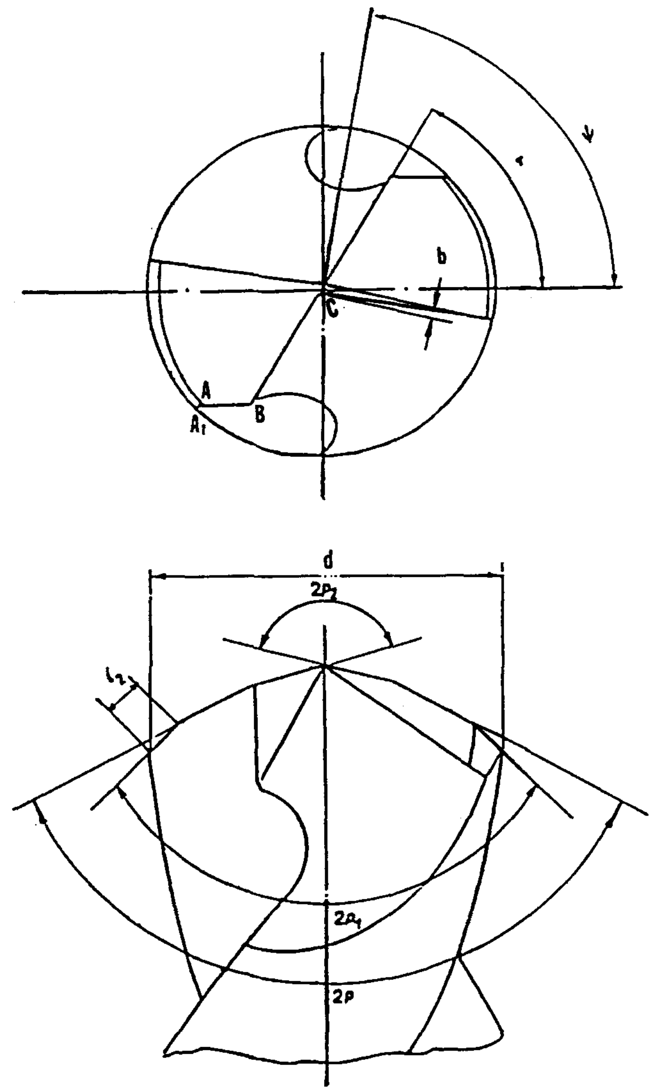

Fig. 6 Optimum crankshaft MFD

Appendix

An optimum crankshaft MFD was developed with an optimization program based on force models. This optimum MFD can drastically reduce the drilling thrust and increase the drill life in crankshaft drilling when compared to the conventional split point drill (Ref 16). The configuration of the optimum crankshaft MFD is shown in Fig. 6.

The optimum crankshaft MFD has a split point with an additional facet added to the outer corner of the drill point. It has triple point angles—2ρ, $2\rho_1$, $2\rho_2$,—and three cutting edges—the inner cutting edge, BC; the middle cutting, AB; and the outer cutting edge, A_1A. This MFD is used in drilling experiments of on-line drill wear recognition.

Acknowledgment

This research was partially supported by the CSU Scholarly and Creative Grants. Supply of work material from the General Motors Corporation is greatly appreciated.

References

1. P.M. Lister and G. Barrow, *Proceedings of the 26th Machine Tool Design and Research Conference*, MacMillian Publishers Limited, 1988, p 271-288
2. T.I. Liu, E.J. Ko, and S.L. Sha, *J. Mater. Shaping Technol.*, Vol 8 (No. 4), ASM International, 1990, p 249-254
3. T. Moriwaki, *Bull. Jpn. Soc. Precis. Eng.*, Vol 18 (No. 2), 1984, p 90-96
4. J.W. Lee, Ph. D. thesis, University of Wisconsin-Madison, 1986
5. T.I. Liu and S.M. Wu, *J. Eng. Ind.*, 1990, ASME, p 299-302
6. K. Subramanian and N.H. Cook, "Sensing of Drill Wear and Prediction of Drill Life," paper No. 76-WA/Prod-33, ASME, 1976
7. K.E. Yee and D.S. Blomquist, "An On-line Method of Determining Tool Wear by Time Domain Analysis," paper No. MR82-901, SME, 1982
8. K.W. Yee, "On the Use of Drill-up for On-Line Determination of Drill Wear," paper No. MS84-914, SME, 1984
9. J.J. Hopfield and D.W. Tank, *Science*, Vol 233, 1986, p 625-633
10. T. Kohonen, *Neural Networks*, Vol 1, 1988, p 3-16
11. D. Rumelhart and J. McClelland, "Parallel Distributed Processing," MIT Press, 1986
12. I. Aleksander, "Artificial Vision for Robotics," U.K., Kogan Page Publ., 1983
13. G. Chryssolouris and M. Guillot, *Proceedings of ASME Winter Annual Meeting Symposium on Sensors and Controls for Manufacturing*, ASME, 1988, p 199-206
14. S. Rangwala and D. Dornfeld, *IEEE Transactions on Systems, Man, Cybernetics*, Vol 19 (No. 2), 1989
15. S. Rangwala and D. Dornfeld, *Proceedings of ASME Winter Annual Meeting Symposium on Intelligent and Integrated Manufacturing Analysis and Synthesis*, ASME, 1987, p 109-120
16. T.I. Liu and S.M. Wu, *J. Mater. Eng. Perform.*, Vol 2 (No. 3), ASM International, 1993, p 571-578